IEEE Access
Multidisciplinary | Rapid Review | Open Access Journal

Received December 21, 2018, accepted January 30, 2019, date of publication February 7, 2019, date of current version February 27, 2019.

Digital Object Identifier 10.1109/ACCESS.2019.2898181

User-Centric Blind Interference Alignment Design for Visible Light Communications

AHMAD ADNAN-QIDAN, (Student Member, IEEE), MÁXIMO MORALES CÉSPEDES, (Member, IEEE), AND ANA GARCÍA ARMADA, (Senior Member, IEEE)
Department of Signal Theory and Communications, Universidad Carlos III de Madrid, 28911 Leganés, Spain

Corresponding author: Ahmad Adnan-Qidan (ahmadq@tsc.uc3m.es)

This work was supported by the Spanish National Project TERESA-ADA (MINECO/AEI/FEDER, UE) under Grant TEC2017-90093-C3-2-R.

ABSTRACT Visible light communications (VLC) are considered as a key technology for future wireless communications. In order to mitigate the interference, several transmit precoding (TPC) schemes have been proposed for VLC. However, beyond the need for channel state information and backhaul links, the TPC schemes are subject to additional constraints given by the features of the optical channel such as ensuring a real and non-negative transmitted signal or a low correlation among users. Besides, the traditional network-centric (NC) design, i.e., considering only the position of the transmitters, leads to rigid transmission schemes for VLC networks due to the small and confined coverage of the optical transmitters.In this paper, we consider blind interference alignment (BIA) schemes for VLC, which solve the aforementioned issues, based on the concept of reconfigurable photodetector. In this context, we propose a user-centric (UC) clustering strategy based on the K-means algorithm where the users are treated as an active element of the network instead of a mere endpoint. For the proposed UC design, we derive two BIA schemes based on the connectivity of the clusters; a straightforward scheme considering each cluster as a broadcast channel referred to as KM-sBIA and a scheme that is flexible to the connectivity of each user within the cluster referred to as KM-topBIA. The simulation results show that the proposed schemes outperform the use of classical TPC or other BIA-based schemes considering both NC and UC approach.

INDEX TERMS Blind interference alignment, K-means, optical wireless, user-centric cluster formation, visible light communications.

I. INTRODUCTION

Owing to the continuous demand on wireless data traffic the use of alternative spectrum bands other than the traditional radio-frequency (RF) communications has been proposed during the last years. In this context, visible light communications (VLC) have received significant attention because of the huge unlicensed bandwidth available in the optical domain. Based on the wide deployment of commercially available Light-Emitting Diode (LED) lights VLC is considered as a key component for future wireless communications [1], [2].

For VLC each transmitter provides coverage within a confined area and employs intensity modulation (IM) and direct detection (DD). Hence, the signal detection is not subject to small scale propagation effects. From the network perspective, each optical transmitter can be considered as a small access point (AP), usually denoted as *attocell* [3]. Furthermore, several LED lamps are usually deployed on the ceiling for providing satisfactory illumination. Therefore, considering several users in the network, VLC naturally configures a multi-user multiple-input multiple-output (MU-MIMO) system [4]. The management of the multi-user interference (MUI) and the intercell interference while avoiding the orthogonal resource allocation in MU-MIMO systems is a problem often found also in the RF systems. In this sense, several transmit precoding (TPC) schemes based on cooperation among transmitters and knowledge of the channel state information (CSI) at the transmitter have been proposed for maximizing the Degrees of Freedom (DoF), i.e., the multiplexing gain [5], [6].

The associate editor coordinating the review of this manuscript and approving it for publication was Minho Jo.

In this context, TPC schemes such as minimizing the mean square error (MMSE) [7], zero-forcing (ZF) [8], [9] or block diagonalization (BD) [10] have been proposed for VLC systems. Beyond the need for CSI at the transmitter or the design of backhaul links, which results also challenging for RF systems, the use of TPC schemes for VLC is not straightforward due to the features of the propagation of the visible light. First, the transmitted signal must be real and non-negative. Since the precoding matrices of the TPC schemes require negative values to cancel or mitigate the interference, a bias current is usually required to be added to the transmitted signal. However, out of the linear region of the LED lights this approach generates clipping distortion [11]. Secondly, because of the lack of small scale effects, the channel responses among the users can be highly correlated, handicapping the performance of the aforementioned TPC schemes [12].

A transmission scheme referred to as blind interference alignment (BIA) was proposed as a means of achieving a growth in DoF without CSI at the transmitter in [13] and [14]. BIA is based on exploiting the channel correlation structure of the users over a coherence period. In [14], the use of reconfigurable antennas is proposed for its implementation in RF systems. Several BIA schemes have been proposed for cellular networks [15], providing diversity [16] or managing the coherence requirements [17]. At this point, it is interesting to remark that the BIA schemes result useful for VLC systems because of features such as

- No need for CSI at the transmitter side.
- No cooperation among the LED lights is required avoiding the deployment of high-data rate backhauls.
- The precoding matrices that determine the transmitted signal are strictly composed of $\{0, 1\}$ values, which ensures the non-negativity of the transmitted signal without the need for a DC bias current.
- The performance of BIA schemes is not subject to the correlation among the channel response of the users.

In [18], a reconfigurable photodetector is proposed for the implementation of BIA in VLC. Basically, it is composed of several photodiodes allocated in an angle diversity structure, e.g., [19], [20], connected to a single signal processing chain through a selector. It is shown that the BIA schemes achieve a similar, or even greater, performance than TPC schemes and improve the fairness and reliability for the broadcast channel (BC) or the homogeneous cellular VLC networks. However, as also occurs for TPC schemes, the BIA approach proposed in [18] does not result suitable for complex VLC networks where a considerable number of optical transmitters and users, e.g., greater than 4 transmitters and users, are deployed in a small area. Specifically, it can lead to low data rates and a demand on channel coherence and signal-to-noise ratio (SNR) challenging to satisfy.

Typically, the complexity and the requirements of any network such as the coherence time, the SNR, the number of users, etc. are managed following a network centric (NC) approach that determines the cell planning, the resource management or the signal processing. However, for small cell networks the NC approach fails to provide a suitable performance. In [21], a novel approach considering flexible strategies for the cell management such as liquid cell, soft cells, or phantom cells is proposed. Applied to VLC, the concept of user centric (UC) design where each user is treated as an active element of the network instead of a simple endpoint is presented in [22] and [23]. A detailed overview of the UC design in comparison to the traditional NC approach is presented in [24]. In [25], the formation of UC clusters is proposed jointly with the use of TPC schemes. However, the TPC schemes are subject to several constraints for VLC as commented above. Managing these constraints leads to a multi-user scheduling (MUS) strategy that affects to the overall performance of the network. In this sense, the TPC schemes are non-flexible and result less suitable for VLC in comparison with BIA.

In this work we propose the use of BIA for VLC networks based on both NC and UC approaches. First, we introduce the implementation of traditional BIA schemes for VLC based on the reconfigurable photodetector proposed in [18]. The application of a NC design improves the performance and utility of traditional BIA schemes with respect to the case of treating the VLC network as a BC comprising the whole set of transmitters and users. Although the NC design improves the performance of BIA, it results too rigid for VLC networks as occurs for TPC schemes. Furthermore, the use of the reconfigurable photodetector provides a wide field-of-view (FoV) for each user ensuring Line-of-Sight (LoS) communication to most of the optical transmitters. As a consequence, the implementation of a UC design does not result straightforward considering transmission based on BIA. The main contributions of this paper are

- We derive a UC clustering strategy based on the K-means algorithm for the implementation of BIA in VLC.
- A scheme referred to as KM-sBIA that implements BIA in each of the UC clusters as a BC is formulated.
- Taking into consideration the connectivity of each user within the corresponding UC cluster, we derive an adaptive scheme referred to as KM-topBIA.

Simulation results show that the proposed UC clustering strategy improves the performance of the NC approach regardless of the transmission scheme. The derived BIA schemes outperform the user rate of TPC or diversity schemes such as ZF or maximum ratio combining (MRC). Moreover, KM-topBIA achieves greater sum-rate than traditional BIA schemes and provides a satisfactory bit error rate (BER) for usual values of optical power while reducing the coherence time requirements.

The remainder of this paper is organized as follows. In Section II we describe the system model. In Section III we describe a cluster formation strategy for a UC design. In Section IV we present a brief overview of BIA to introduce some useful concepts. After that, the implementation of BIA following a NC approach is described in Section V. Section VI presents a novel variation of BIA for the UC design. Section VII presents some simulation

results. Finally, Section VIII provides some concluding remarks.

Notation. The following notation is considered in this work. Bold upper case and lower case letters denote matrices and vectors, respectively, $\mathbf{I}_M$ and $\mathbf{0}_M$ denote the $M \times M$ identity and zero matrices, respectively, while $\mathbf{0}_{M,N}$ corresponds to the $M \times N$ zero matrix, $\mathbf{1}_M$ is the $M \times 1$ all ones vector, $\otimes$ represents the Kronecker product, $[\ ]^T$ and $[\ ]^H$ are the transpose and the hermitic transpose operators, respectively, $\mathbb{E}$ is the statistical expectation and col{} is the column operator that stacks the considered vectors in a column.

II. SYSTEM MODEL

We consider an indoor VLC system where L, $l = \{1, \ldots, L\}$, optical transmitters composed of a single LED are distributed uniformly on the ceiling. The set of L transmitters provides illumination and data transmission to K, $k = \{1, \ldots, K\}$, users randomly distributed and equipped with a reconfigurable photodetector as proposed in [18]. The reconfigurable photodetector provides M, $m = \{1, \ldots, M\}$, linearly independent channel responses to each user denoted as preset modes. The user k selects a single preset mode at time n. The transmitted signal can be written in a vector form as $\mathbf{x} = [x_1, \ldots, x_L] \in \mathbb{R}_+^{L\times 1}$. Thus, the signal received by the user k corresponding to the preset mode m at time n is

$$y^{[k]}[n] = \mathbf{h}^{[k]}\left(m^{[k]}[n]\right)^T \mathbf{x}[n] + z^{[k]}[n], \tag{1}$$

where $\mathbf{h}^{[k]}\left(m^{[k]}[n]\right) \in \mathbb{R}_+^{L\times 1}$ is the channel vector between the L optical transmitters and the user k for the preset mode m selected at time n and $z^{[k]}[n]$ is real valued additive white Gaussian noise (AWGN) with zero mean and variance σ_z^2 considering the shot and thermal noise [26].

We assume that the pattern functions of each user $m^{[k]}[n]$ are predetermined and known beforehand. Moreover, we consider that the reconfigurable photodetector of each user can provide $M \geq L$ preset modes. On the contrary, the LED transmitters do not have any CSI or cooperation among them and each transmitter does not have more information than the coherence time of the network. In the following, we describe the set-up of the VLC system.

A. TRANSMITTER

The transmitted signal must be a non-negative real value. Satisfying this constraint for TPC schemes involves to add a bias current that counterbalances the negative values given by the precoding. However, the original signal can suffer clipping distortion if the bias current does not overcome the negative values. Notice that BIA naturally satisfies this constraint since the precoding matrices are composed of {0, 1} values. On the other hand, the output optical power is only linear over a limited drive current range $[I_L, I_H]$ where I_L is the turn on current of the LED and I_H corresponds to the maximum input that ensures both the linear response of the LED. Within this range, each LED provides an optical power $[0, P_{\max}]$.

In this work, we consider N-ary pulse amplitude modulation (N-PAM) where the mean of the transmitted signal is equal to the current that provides the desired illumination intensity. Thus, each symbol can take N possible values within the range $[0, I_H]$. For instance, in a 4-PAM each symbol can take any value of the set $(I_H - I_L) \times \left\{0, \frac{1}{3}, \frac{2}{3}, 1\right\} + I_L$.[1] Therefore, the average of the transmitted signal is $\mathbb{E}[s] = I_{\text{avg}}$, which generates the desired optical power P_{avg}.

B. CHANNEL MODEL

For VLC the channel is composed of a LoS component corresponding to the direct transmission from the LED to the user and a diffuse component because of the reflection on walls, floor and ceiling. In [27], it is revealed that the LoS component represents more than the 95% of the received optical power. Since the reconfigurable photodetector provides a wide FoV, the LoS propagation constitutes the most important contribution of the channel considering that the diffuse component is negligible.

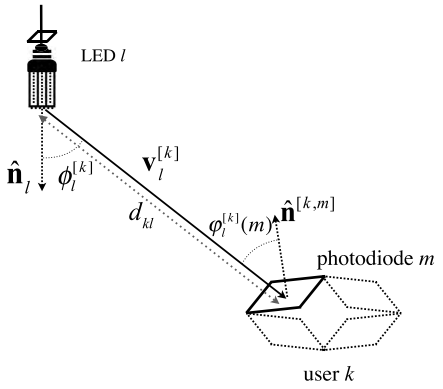

FIGURE 1. Geometry of the considered setting comprising the irradiance and the incidence angles for the transmitter-photodiode pair. Each photodiode provides a preset mode of the reconfigurable photodetector of user k.

The LoS component is given by the geometry of the pair transmitter-receiver as is shown in Fig. 1. The distance between the transmitter l and the receiver k is denoted as d_{kl} and the angles of irradiance[2] and incidence for the preset mode m, $m = \{1, \ldots, M\}$, are denoted as $\phi_l^{[k]}$ and $\varphi_l^{[k]}(m)$, respectively. Thus, the LoS component [26] between the user k and the transmitter l at the preset mode m is given by (2), as shown at the bottom of the next page, where δ and A are the responsivity and the area of detection of the photodiode, respectively, $g\left(\varphi_l^{[k]}(m)\right)$ is the gain of the optical filter and the concentrator, r is the coefficient of the photodiode, Ψ_F denotes the FoV of the photodiode and $R_0(\phi_l^{[k]})$ denotes the Lambertian radiation intensity given by $R_0 = \frac{t+1}{2\pi}\cos^t(\phi_l^{[k]})$ where $t = \frac{-\ln 2}{\ln(\cos(\phi_{1/2}))}$ is the Lambertian emission and $\phi_{1/2}$ is the transmitter semiangle.

[1] Notice that other values between 0 and 1 can be considered.

[2] Assuming that the size of the photodiodes is much smaller than the distance to any light transmitter, the irradiance angle between any photodiode of the user k and the transmitter l can be approximated as $\phi_l^{[k]}(m) \approx \phi_l^{[k]}$.

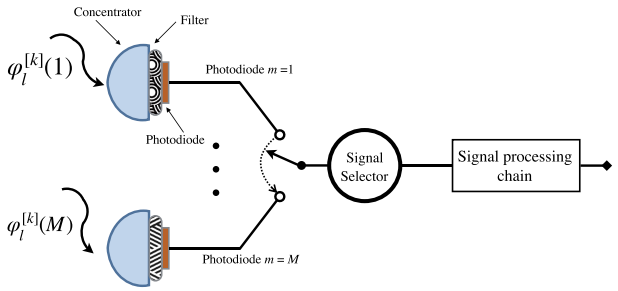

FIGURE 2. Structure of the reconfigurable photodetector.

C. RECEIVER

We present a brief overview of the reconfigurable photodetector [18]. Typically, the photodiodes of each user are orientated perpendicularly upwards. This configuration can generate correlated channel responses among the users. In contrast, the reconfigurable photodetector is composed of several photodiodes in an angle diversity configuration where each photodiode provides a distinct receiving orientation angle (ROA). The set of photodiodes is connected to a single signal processing chain through a selector as is shown in Fig. 2.

The orientation of the photodiode m of the reconfigurable photodetector of the user k is given by its polar and azimuthal angles denoted as $\theta^{[k,m]}$ and $\alpha^{[k,m]}$, respectively. Thus, the orientation vector of the photodiode m of the user k is

$$\hat{\mathbf{n}}^{[k,m]} = \Big[\sin(\theta^{[k,m]})\cos(\alpha^{[k,m]}), \sin(\theta^{[k,m]})\sin(\alpha^{[k,m]}), \cos(\theta^{[k,m]})\Big]. \quad (3)$$

The irradiance and the incidence angles are determined by

$$\phi_l^{[k]} = \arccos\left(\frac{\hat{\mathbf{n}}_l \mathbf{v}_l^{[k]}}{\|\hat{\mathbf{n}}_l\|\|\mathbf{v}_l^{[k]}\|}\right) \quad (4)$$

$$\varphi_l^{[k]}(m) = \arccos\left(\frac{\hat{\mathbf{n}}^{[k,m]} \mathbf{v}_l^{[k]}}{\|\hat{\mathbf{n}}^{[k,m]}\|\|\mathbf{v}_l^{[k]}\|}\right) \quad (5)$$

respectively, where $\hat{\mathbf{n}}_l$ is the normal orientation vector of the transmitter l and $\mathbf{v}_l^{[k]}$ is the vector from the transmitter l to the user k. For transmitters pointing to the floor $\hat{\mathbf{n}}_l = [0, 0, 1]$.

A geometrical pattern can be applied for the arrangement of the photodiodes with the aim of providing distinct and linearly independent channel responses [19]. For instance, a pyramidal arrangement considers the same azimuthal angle, i.e., $\theta^{[k,m]} = \theta_{\text{pyr}}$ while the polar angle of the photodiode m of the user k is $\alpha^{[k,m]} = \frac{2(m-1)\pi}{M}$, $m = \{1, \ldots, M\}$. Furthermore, notice that other arrangements such as hemispherical or random ROA distributions can be easily proposed.

III. CLUSTER FORMATION

Following a similar notation as [25], the VLC network is defined as a bipartite graph $\mathcal{G}(\mathcal{V}, \mathcal{E})$. The set of vertex $\mathcal{V}$ contains the nodes that compose the network. Hence, it can be divided into two subsets; $\mathcal{V}_\mathcal{L}$ for the optical transmitters and $\mathcal{V}_\mathcal{K}$ for the users. That is,

$$\mathcal{V} = \mathcal{V}_\mathcal{L} \cup \mathcal{V}_\mathcal{K} = \{l = 1, 2, \ldots, L\} \cup \{k = 1, 2, \ldots, K\}, \quad (6)$$

where l and k denote the index of the optical transmitters and the users, respectively. In contrast to [25], we consider a topological approach where a link may be stablished between a pair transmitter-receiver when the average received power exceeds a determined threshold given by the distance between transmitter and receiver, which is denoted as d_{th}. The signal received from all other transmitters below this threshold is treated as noise. Therefore, the edge set $\mathcal{E}$ that contains the possible links between the optical transmitters and the users, i.e., between the elements of $\mathcal{V}_\mathcal{L}$ and $\mathcal{V}_\mathcal{K}$ is

$$\mathcal{E} = \left\{e_{l,k} / \text{dist}\,(l, k) \leq d_{\text{th}}, l \in \mathcal{V}_\mathcal{L}, k \in \mathcal{V}_\mathcal{K}\right\}, \quad (7)$$

where $e_{l,k}$ is the link between the transmitter l and the user k and dist(a, b) denotes the distance between a and b.

A. NETWORK CENTRIC APPROACH

For traditional RF networks clustering is based on a NC approach where a careful deployment of base stations (BSs) is organized in clusters subject to a frequency reuse strategy (FR) [28]. Thus, transmission for neighbouring clusters occurs in distinct bandwidths avoiding the interference among them. However, there exists inter-tier interference among clusters operating in the same bandwidth. Within each cluster interference because of transmission to multiple users is managed through TPC or orthogonal resource allocation schemes. This network centric (NC) approach generates static clusters independently of the user distribution. In this sense, although the NC approach has been successful for RF cellular networks, it does not result suitable for VLC where each transmitter comprises a small size and confined coverage area.

Assigning distinct frequency bands to neighbouring transmitters leads to a frequency handover every few meters, which results unpractical in the optical domain [29]. Considering a NC approach the transmitters of the VLC network are divided into uniform clusters. For instance, dividing the scenario shown in Fig. 3 into four uniform clusters. Notice that managing the interference among the users belonging to the same cluster is simplified considerably in comparison to managing the whole network over the same bandwidth. However, this approach involves to divide the bandwidth into

$$h_l^{[k]}(m) = \begin{cases} \dfrac{\delta A}{d_{kl}^2} R_0\left(\phi_l^{[k]}\right) g\left(\varphi_l^{[k]}(m)\right) \cos^r\left(\varphi_l^{[k]}(m)\right) & \text{if } \varphi_l^{[k]}(m) \leq \Psi_F \\ 0 & \text{if } \varphi_l^{[k]}(m) \geq \Psi_F, \end{cases} \quad (2)$$

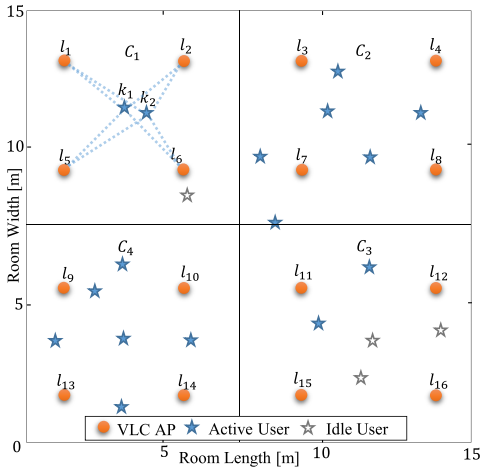

FIGURE 3. Cluster formation based on the NC approach. The deployment of optical transmitters comprises four uniform square clusters.

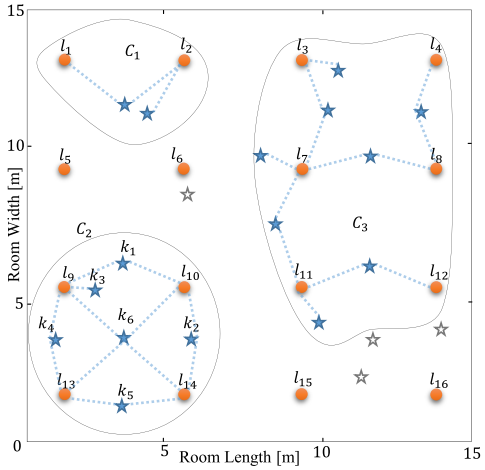

FIGURE 5. Cluster formation based on the proposed UC clustering algorithm.

four parts assigning each to a cluster. As a consequence, the achievable sum-rate is divided also by four. Moreover, considering the distribution of the active users, a NC approach generating uniform clusters results too rigid for VLC networks.

B. USER CENTRIC APPROACH

For illustrative purposes we consider a VLC network composed of $L = 4$ transmitters as is shown in Fig. 4 to introduce the UC approach. Since each optical transmitter illuminates an independent cell, intercell interference appears at the cell edge represented by shaded areas in Fig. 4(a). In order to mitigate the intercell interference, the optical transmitters form a cluster as is shown in Fig. 4(b) for a NC design. However, as commented above, this approach results too rigid for VLC. Motivated by the UC approach proposed in [22] and [25], we consider the formation of irregular-shape clusters as is shown in Fig. 4(c). In contrast to the aforementioned works, we consider a UC approach based on the network topology with the aim of implementing BIA schemes.

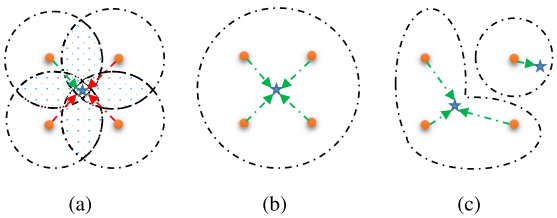

FIGURE 4. Cluster formation for a toy example. (a) Independent transmission per each cell. No clustering (b) NC approach, (c) UC approach.

In this work, we propose a UC design based on the K-means algorithm to determine the formation of elastic clusters [30]. Let us first introduce some common notation. The number of the considered clusters is denoted as C and each cluster $c, c = \{1, \ldots, C\}$, is denoted as $\mathcal{C}_c = \mathcal{V}_{\mathcal{L}_c} \cup \mathcal{V}_{\mathcal{K}_c}$ where $\mathcal{V}_{\mathcal{L}_c}$ and $\mathcal{V}_{\mathcal{K}_c}$ are the set of transmitters and users that compose the cluster c, respectively. Thus, the proposed methodology is given by the following steps

1) Determine the number of clusters

In general, there is no method for determining the optimal number of clusters. Notice that the complexity of the interference management is reduced as C increases since each cluster considers less transmitters and users. On the other hand, a reduced number of clusters involves to increase the sources of inter-cluster interference. Therefore, there exists an optimal value of C that provides a trade-off between the efficiency of the interference management within each cluster and the inter-cluster interference. In this sense, considering the low mobility of the users for VLC, the optimal value can be determined within a sufficient short period through a heuristic search.

2) USER SET FORMATION

Once the number of clusters is known, the algorithm determines the set of inactive users denoted as $\mathcal{V}_{\mathcal{K},idle}$ and the set of active users $\mathcal{V}_{\mathcal{K}}$. As a consequence, the inactive users are not considered in the clustering strategy. If a user k becomes active that user is removed from $\mathcal{V}_{\mathcal{K},idle}$ and assigned to $\mathcal{V}_{\mathcal{K}}$.

The K-means algorithm is based on partitioning the set of $\mathcal{V}_{\mathcal{K}}$ active users into C clusters. The starting point of each cluster is the location of user $k \in \mathcal{V}_K$ given by (x_k, y_k) where (x_k, y_k) determines the position of the user k in the receiving plane. The centroid of the cluster c at the i-th iteration of the clustering algorithm is denoted as $\xi_c(i)$ given by the coordinates $(x_{\xi_c(i)}, y_{\xi_c(i)})$. During the first iteration the centroid of the C clusters is determined by the location of C users belonging to $\mathcal{V}_{\mathcal{K}}$ selected randomly. Once the centroids are determined, during the i-th iteration each user is assigned to the closest centroid, that is

$$k = \arg\min_{k \in \mathcal{V}_{\mathcal{K}}} \ \text{dist}(\xi_c(i), k), \tag{8}$$

	1	2	3
User 1	$\mathbf{h}^{[1]}(1)$	$\mathbf{h}^{[1]}(2)$	$\mathbf{h}^{[1]}(1)$
User 2	$\mathbf{h}^{[2]}(1)$	$\mathbf{h}^{[2]}(1)$	$\mathbf{h}^{[2]}(2)$

FIGURE 6. Supersymbol for sBIA. BC with $L = 2$ and $K = 2$.

where $\text{dist}(\xi_c(i), k)$ is the Euclidean distance between the user k and the tentative cluster centroid $\xi_c(i)$, i.e., $\text{dist}(\xi_c(i), k) = \sqrt{(x_k - x_{\xi_c(i)})^2 + (y_k - y_{\xi_c(i)})^2}$. If there are more than one user satisfying the equation (8) during the iteration i, only one of them is randomly assigned to the cluster. After that, the position of the centroids are updated according to the position of the selected users

$$\xi_c(i) = \left(\frac{x_{\xi_c(i)} + x_k}{2}, \frac{y_{\xi_c(i)} + y_k}{2} \right). \tag{9}$$

The set of users belonging to $\mathcal{V}_{\mathcal{K}_c}$ is determined by iteratively applying equation (8) until the position of the centroids does not change significantly.

3) TRANSMITTERS SET FORMATION

To complete the formation of the clusters, the set of transmitters assigned to the cluster c must be determined. According to the proposed topological approach (see (7)) a transmitter l belongs to the cluster c if the distance is lower than the threshold d_{th}. That is,

$$\mathcal{V}_{\mathcal{L}_c} = \{ l \,/\, \text{dist}\,(l, \xi_c) \leq d_{th} \}, \tag{10}$$

where the location of the transmitter l is denoted as (x_l, y_l) and ξ_c is the centroid of the cluster c after concluding the K-means algorithm. Notice that this criterion is defined by the distance between the cluster centroid and each transmitter. Therefore, there can exist users with distinct connectivity, i.e., connected to a different number of transmitters, within each cluster. Moreover, we consider that there is no overlap between the transmitters of distinct clusters, i.e., $\mathcal{V}_{\mathcal{L}_c} \cap \mathcal{V}_{\mathcal{L}_{c'}} = \emptyset$, $c \neq c'$. If a transmitter l^* belongs to several subsets $\mathcal{V}_{\mathcal{L}_c}$ it is assigned to the cluster c that satisfies

$$l^* \in \mathcal{V}_{\mathcal{L}_c} \,/\, \arg\min_c \text{dist}\left(l^*, \xi_c\right). \tag{11}$$

The algorithm concludes when C clusters are successfully constructed by forming unique $\mathcal{V}_{\mathcal{L}_c}$ and $\mathcal{V}_{\mathcal{K}_c}$ sets where $\mathcal{V}_{\mathcal{L}_c} \cap \mathcal{V}_{\mathcal{L}_{c'}} = \emptyset$, $\mathcal{V}_{\mathcal{K}_c} \cap \mathcal{V}_{\mathcal{K}_{c'}} = \emptyset$ and $c \neq c'$.

IV. BLIND INTERFERENCE ALIGNMENT

For the sake of a clear explanation, let us first present a brief overview of the BIA scheme presented in [14] for the BC referred to as standard BIA (sBIA) from now on.

A. TOY EXAMPLE. $L = 2$ OPTICAL TRANSMITTERS AND $K = 2$ USERS

For illustrative purposes, we first consider a simple setting comprising $L = 2$ transmitters and $K = 2$ users. The pattern of preset modes selected by each user, referred to as *supersymbol* from now on, is shown in Fig. 6 and the transmitted signal is given by

$$\mathbf{X} = \begin{bmatrix} \mathbf{x}[1] \\ \mathbf{x}[2] \\ \mathbf{x}[3] \end{bmatrix} = \underbrace{\begin{bmatrix} \mathbf{I}_2 \\ \mathbf{I}_2 \\ \mathbf{0}_2 \end{bmatrix}}_{\mathbf{W}^{[2]}} \mathbf{u}^{[1]} + \underbrace{\begin{bmatrix} \mathbf{I}_2 \\ \mathbf{0}_2 \\ \mathbf{I}_2 \end{bmatrix}}_{\mathbf{W}^{[1]}} \mathbf{u}^{[1]} \tag{12}$$

where $\mathbf{u}^{[k]} = \left[u_1^{[k]}, u_2^{[k]} \right]^T$ is the symbol intended to the user k and $u_l^{[k]}$ is the symbol transmitted by the transmitter l to the user k. Moreover, $\mathbf{W}^{[k]}$ denotes the precoding matrix of the user k. It can be seen that the supersymbol comprises two parts; the Block 1 where both symbols are transmitted simultaneously and Block 2 during which each symbol is transmitted in orthogonal fashion, i.e., in a dedicated symbol extension.

Focussing on the user 1, the signal received during the entire supersymbol is

$$\begin{bmatrix} y^{[1]}[1] \\ y^{[1]}[2] \\ y^{[1]}[3] \end{bmatrix} = \underbrace{\begin{bmatrix} \mathbf{h}^{[1]}(1)^T \\ \mathbf{h}^{[1]}(2)^T \\ \mathbf{0}_{2,1}^T \end{bmatrix}}_{\text{rank=2}} \mathbf{u}^{[1]} + \underbrace{\begin{bmatrix} \mathbf{h}^{[1]}(1)^T \\ \mathbf{0}_{2,1}^T \\ \mathbf{h}^{[1]}(1)^T \end{bmatrix}}_{\text{rank=1}} \mathbf{u}^{[2]} + \begin{bmatrix} z^{[1]}[1] \\ z^{[1]}[2] \\ z^{[1]}[3] \end{bmatrix}. \tag{13}$$

The symbol $\mathbf{u}^{[1]}$ is contained in a 2-rank matrix while the interfering symbol $\mathbf{u}^{[2]}$ is aligned in a 1-rank matrix. Thus, the user 1 can measure the interference because of transmission to the user 2 at the third symbol extension and remove it afterwards. The signal after interference subtraction is

$$\begin{bmatrix} y^{[1]}[1] - y^{[1]}[3] \\ y^{[1]}[2] \end{bmatrix} = \underbrace{\begin{bmatrix} \mathbf{h}^{[1]}(1)^T \\ \mathbf{h}^{[1]}(2)^T \end{bmatrix}}_{\mathbf{H}^{[1]}} \mathbf{u}^{[1]} + \begin{bmatrix} z^{[1]}[1] - z^{[1]}[3] \\ z^{[1]}[2] \end{bmatrix}. \tag{14}$$

Since each preset mode of the reconfigurable photodetector provides a linearly independent channel response, $\mathbf{H}^{[1]}$ is a full rank channel matrix, and therefore, the symbol $\mathbf{u}^{[1]}$ can be decoded by solving the equation system given by (14) only subject to noise addition. Moreover, notice that a noise increase appears because of the interference subtraction.

The sBIA scheme provides 2 DoF during 3 symbol extensions to the user 1 for the considered setting. Similarly, the user 2 obtains 2 DoF by measuring the interference during the second symbol extension. Therefore, $\frac{4}{3}$ sum-DoF are achievable. It is interesting to remark that orthogonal transmission obtains a sum-DoF equal to 1.

B. GENERAL CASE. BC WITH L OPTICAL TRANSMITTERS AND K USERS

The key idea behind BIA is to create a supersymbol and a transmission structure based on the following criterion; *the channel state of the user k varies among L preset modes during the transmission of the intended symbol while the*

channel state of all other users $k' \neq k$ remains constant [14]. *The symbol extensions of the user k that satisfy this criterion are referred to as an alignment block from now on.*

For the general case, the sBIA supersymbol is constructed systematically creating *alignment blocks*. Since several alignment blocks can be allocated to each user, we denote the symbol transmitted during the alignment block ℓ to the user k as $\mathbf{u}_\ell^{[k]} \in \mathbb{R}^{L\times 1}$. The first $L-1$ symbol extensions of each alignment block correspond to the Block 1 while the last symbol extension corresponds to the Block 2. The construction of the Block 1 for sBIA follows the structure shown in Fig. 7. It can be seen that this methodology generates $(L-1)^{K-1}$ alignment blocks for each user. Hence, the length of Block 1 for sBIA comprises $(L-1)^K$ symbol extensions. Notice that the transmission of the symbol $\mathbf{u}_\ell^{[k]}$, $\ell = 1, \ldots, (L-1)^{K-1}$, is carried out in groups, which determine the structure of the transmitted signal. After that, in Block 2, each symbol $\mathbf{u}_\ell^{[k]}$ is transmitted in orthogonal fashion satisfying the BIA criterion, i.e., completing the alignment block with the preset mode L. Thus, the Block 2 comprises $K(L-1)^{K-1}$ symbol extensions. The temporal correlation function that determines the preset mode selected at time n by the user k for the sBIA scheme, and therefore, the supersymbol structure, is denoted as $f^{[k]}(n)$. Moreover, it can be differentiated between $f_{\text{B1}}^{[k]}(n)$ and $f_{\text{B2}}^{[k]}(n)$ for the Block 1 and Block 2, respectively. Similarly, the precoding matrix for the user k is denoted as $\mathbf{W}^{[k]} = \left[\mathbf{W}_{\text{B1}}^{[k]^T}\ \mathbf{W}_{\text{B2}}^{[k]^T}\right]^T$ where $\mathbf{W}_{\text{B1}}^{[k]}$ and $\mathbf{W}_{\text{B2}}^{[k]}$ are the precoding matrices for the Block 1 and Block 2, respectively.

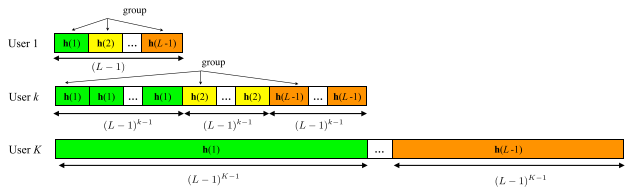

FIGURE 7. Systematic construction of the Block 1 for sBIA. Each color represents a preset mode.

Cancelling the interference in sBIA is based on measuring the interference during Block 2, in which each symbol is transmitted in a dedicated symbol extension, and subtracting it afterwards from the polluted symbol extensions in Block 1. For the considered example shown in Fig. 6, it can be easily checked that the symbol extensions $\{1, 2\}$ and $\{1, 3\}$ form an alignment block for the users 1 and 2, respectively. For the general case this methodology is as shown in Fig. 8. The first $L-1$ symbol extensions of the Block 1 and the first symbol extensions of Block 2 form an alignment block. Focussing on transmission of $\mathbf{u}_1^{[k]}$, notice that it is contained in a full rank matrix for user k, i.e., comprises L preset modes, while all other users $k' \neq k$ can measure the interference because of transmission of $\mathbf{u}_1^{[k]}$ at the first symbol extension of Block 2. Satisfying the BIA criterion ensures that the interference is contained in a single preset mode for all other users. Therefore, the interference due to the transmission of

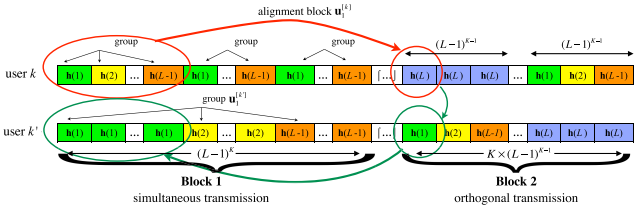

FIGURE 8. Example of alignment block and interference measurement and subtraction. Each color represents a preset mode.

$\mathbf{u}_1^{[k]}$ can be measured at the same channel state where this symbol interferes in Block 1 for all other users $k' \neq k$.

Considering a BC with L transmitters and K users, the sBIA scheme provides $(L-1)^{K-1}$ alignment blocks per user providing L DoF each. Thus, the entire supersymbol comprises

$$\Lambda_{\text{sBIA}} = (L-1)^K + K(L-1)^{K-1} \tag{15}$$

symbol extensions. Therefore, the achievable sum-DoF per symbol extension is

$$\text{DoF}_{\text{sBIA}} = \frac{LK(L-1)^{K-1}}{(L-1)^K + K(L-1)^{K-1}} = \frac{LK}{L+K-1}. \tag{16}$$

The achievable rate of the user k for sBIA is [14]

$$R_{\text{sBIA}}^{[k]} = \frac{1}{L+K-1} \times \mathbb{E}\left[\log\det\left(\mathbf{I} + P_{\text{str}}\mathbf{H}^{[k]}\mathbf{H}^{[k]^H}\mathbf{R}_z^{-1}\right)\right], \tag{17}$$

where P_{str} is the optical power allocated to each stream, $\mathbf{H}^{[k]} = \left[\mathbf{h}^{[k]}(1) \ldots \mathbf{h}^{[k]}(L)\right]^T \in \mathbb{R}^{L\times L}$ is the channel matrix of the user k and $\mathbf{R}_z = \begin{bmatrix} K\mathbf{I}_{L-1} & 0 \\ 0 & 1 \end{bmatrix}$.

The sum-DoF of (16) assumes full connectivity between each user and the whole set of transmitters. Besides the supersymbol length grows exponentially as the number of users increases (see (15)). In this sense, although the VLC systems comprise a reduced number of users, this issue can be a limiting factor. Beyond the DoF metric, the noise increase because of the interference subtraction is proportional to the number of users. That is, the SNR requirements are more restrictive as the number of users increases.

V. NETWORK CENTRIC BLIND INTERFERENCE ALIGNMENT

Following a NC design the straightforward strategy is to divide the deployment of LED transmitters into regular and uniform clusters. Notice that these clusters are static and rely on a fixed cell-shape regardless of the user distribution. Thus, the network is composed of C static clusters, $c = \{1, \ldots, C\}$, composed of a fixed number of transmitters $L_c = \frac{L}{C}$ and K_c users each. Each cluster is denoted as $C_c\,(L_c, K_c)$.

Let us consider the network shown in Fig. 3. A simple NC approach consists on dividing the deployment into $C = 4$ regular square clusters comprising $L_c = 4$ LED lights each. Thus, considering the active users, the $C = 4$ clusters

are given by $C_1(4,2)$, $C_2(4,6)$, $C_3(4,2)$ and $C_4(4,6)$. It is interesting to remark that, assuming a TPC scheme, the clusters $c = \{2,4\}$ can only serve L_c users simultaneously since since $L_c < K_c$. As a consequence, a scheduling strategy would be required in these clusters to serve all the users. Assuming full connectivity and applying the sBIA to each cluster, the achievable sum-DoF equals $\frac{8}{5}+\frac{8}{3}+\frac{8}{5}+\frac{8}{3} \approx 8.53$ DoF. However, this approach relies on two conditions; i) the inter-cluster interference can be treated optimally as noise and ii) the users have full connectivity to the whole set of transmitters of the cluster.

For the general case, each cluster implements a sBIA scheme. Thus, assuming that the aforementioned conditions are satisfied, the sum-DoF potentially achievable is

$$\mathrm{DoF}_{\mathrm{NC-sBIA}} = \sum_{c=1}^{C} \frac{L_c K_c}{L_c + K_c - 1}. \tag{18}$$

Besides, the restriction to channel variability is given by the largest supersymbol, during which the physical channel must remain constant. In this sense, the largest supersymbol is

$$\Lambda_{\mathrm{NC-sBIA}} = \max_{c} \left\{ (L_c - 1)^{K_c} + K_c (L_c - 1)^{K_c - 1} \right\}. \tag{19}$$

Since the inter-cluster interference is treated as noise, the signal received during an alignment block ℓ after interference subtraction for the user k of the cluster c is given by

$$\mathbf{y}^{[k,c]} = \mathbf{H}_c^{[k]} \mathbf{u}_\ell^{[k,c]} + \sum_{c'=1, c' \neq c}^{C} \mathbf{H}_{c'}^{[k]} \mathbf{x}_c + \mathbf{z}^{[k,c]}, \tag{20}$$

where $\mathbf{H}_c^{[k]} \in \mathbb{R}^{L_c \times L_c}$ is the channel matrix between the L_c transmitters of the cluster c and the user k, $\mathbf{u}_\ell^{[k,c]}$ is the symbol intended to the user k and $\mathbf{x}_c$ is the signal transmitted by the L_c transmitters that compose the cluster c. Thus, the rate achievable by the user k located within cluster c is given by

$$R_{\mathrm{NC-sBIA}}^{[k,c]} = \frac{1}{L_c + K_c - 1} \times \mathbb{E}\left[\log\det\left(\mathbf{I} + P_{\mathrm{str}} \mathbf{H}_c^{[k]} \mathbf{H}_c^{[k]H} \mathbf{R}_{z_I}^{-1} \right) \right], \tag{21}$$

where the covariance matrix of the noise plus interference is

$$\mathbf{R}_{z_I} = \mathbf{R}_z + \sum_{c'=1, c' \neq c}^{C} P_{\mathrm{led}} \mathbf{H}_{c'}^{[k]} \mathbf{H}_{c'}^{[k]H} \tag{22}$$

and P_{led} is the optical power of the interfering transmitters and $\mathbf{R}_z = \begin{bmatrix} K_c \mathbf{I}_{L_c - 1} & 0 \\ 0 & 1 \end{bmatrix}$.

VI. USER CENTRIC BLIND INTERFERENCE ALIGNMENT

Although the UC design creates flexible clusters with the aim of reducing the inter-cluster interference, it is necessary to manage the interference within each cluster. In the following we propose two alternative BIA schemes for this issue.

A. STANDARD BIA-BASED ON THE UC APPROACH

Since the proposed UC clustering strategy based on the K-means algorithm provides a set of clusters, the straightforward solution is to implement a sBIA scheme in each of these clusters without considering the user distribution inside the cluster. This scheme is referred to as KM-sBIA. It can be easily checked that the derivation of the achievable DoF and rates follows the same equations as derived in Section V. Notice that the goal of this approach is not to increase the achievable DoF but to reduce the inter-tier interference. Indeed, the achievable DoF can decrease depending on the topology while increasing the achievable sum-rate.

The clustering strategy proposed in Section III for $C = 3$ obtains a clustering formation as is shown in Fig. 5. Thus, there are three clusters given by $C_1(2,2)$, $C_2(4,6)$ and $C_3(6,8)$. Considering the use of sBIA in each cluster the sum-DoF that can be potentially achieved according to (16) is $\frac{4}{3} + \frac{24}{9} + \frac{48}{13} \approx 7.69$ DoF. Notice that the sum-DoF is smaller than for the NC approach. However, the achievable rate of the users at the edge of the clusters increases since the inter-cluster interference has been reduced.

B. TOPOLOGICAL BLIND INTERFERENCE ALIGNMENT BASED ON A UC APPROACH. A TOY EXAMPLE

In the following we devise an alternative BIA scheme that exploits the topology of each cluster referred to as KM-topBIA. For illustrative purposes, we first describe the scheme for a toy example and after that we derive the general case.

Once the clustering of the VLC network has been determined, each cluster can be divided into Q, $q = \{1, \ldots, Q\}$, graphs depending on the connectivity of the users. The connectivity graph where all the users are connected to $\tilde{L}_q$ transmitters belonging to the cluster c is defined as $\mathcal{Q}_q = \mathcal{V}_{\mathcal{L}_q} \cup \mathcal{V}_{\mathcal{K}_q}$ where $\mathcal{V}_{\mathcal{L}_q}$ and $\mathcal{V}_{\mathcal{K}_q}$ are the subsets that contain the optical transmitters and the users of the connectivity graph, respectively. The number of transmitters and users that compose the graph $\mathcal{Q}_q$ is denoted as L_q and K_q, respectively. Notice that we omit the cluster index for the sake of simplicity. For instance, the cluster c_2 of the considered toy example whose graph is shown in Fig. 9 comprises 3 connectivity graphs, $\mathcal{Q}_1 = \{l = 9\} \cup \{k = 3\}$, $\mathcal{Q}_2 = \{l = 9, 10, 13, 14\} \cup \{k = 1, 2, 4, 5\}$ and $\mathcal{Q}_3 = \{l = 9, 10, 13, 14\} \cup \{k = 6\}$ for a connectivity to 1, 2, and 4 transmitters, respectively.

The parameters that determine the supersymbol of the KM-topBIA scheme are the connectivity of each graph $\tilde{L}_q$, e.g., $\tilde{L}_1 = 1$, $\tilde{L}_2 = 2$, $\tilde{L}_3 = 4$, and the number of users that cannot reuse the same pattern of preset modes denoted as $\tilde{K}_q$, $\tilde{k}_q = \{1, \ldots, \tilde{K}_q\}$. Basically, if a pair of users belonging to the same connectivity graph do not have any transmitter in common they can reuse the same pattern. Thus, each pattern of preset modes, i.e., the supersymbol of the user $\tilde{k}_q$, comprises the set of users that can reuse that supersymbol, which is denoted as $\mathcal{K}_{\tilde{k}_q} = \{\mathcal{K}_{\tilde{k}_q}(1), \ldots, \mathcal{K}_{\tilde{k}_q}(\eta_{\tilde{k}_q})\}$ where $\eta_{\tilde{k}_q}$ is the reusing factor of the supersymbol for the user $\tilde{k}_q$.

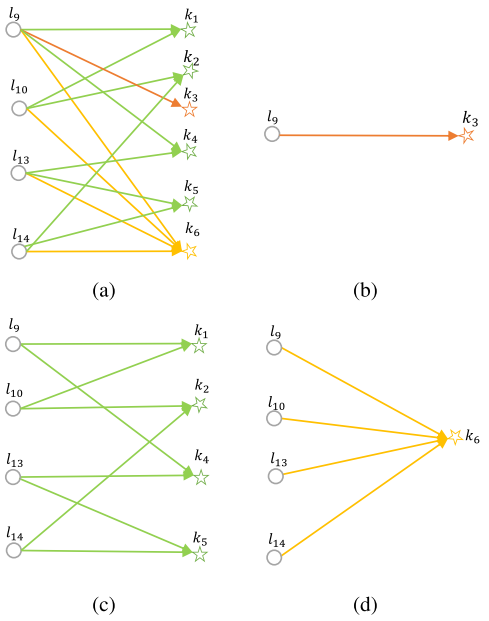

FIGURE 9. (a) Graph of the considered cluster. (b) Connectivity graph $\mathcal{Q}_1$. (c) Connectivity graph $\mathcal{Q}_2$. (d) Connectivity graph $\mathcal{Q}_3$.

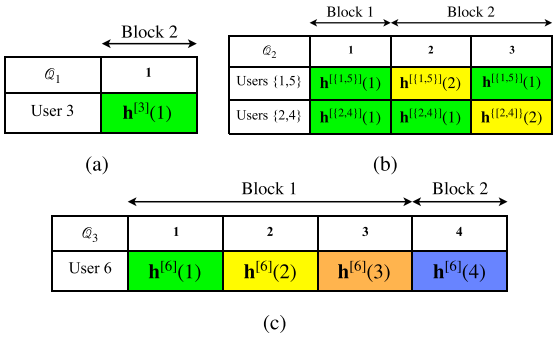

FIGURE 10. a) Supersymbol of the graph $\mathcal{Q}_1$ b) Supersymbol of the graph $\mathcal{Q}_2$, c) Supersymbol of the graph $\mathcal{Q}_3$.

Hence, each user $\tilde{k}_q$ can be treated as a virtual user that defines a pattern of preset modes in which the set of users $\mathcal{K}_{\tilde{k}_q}$ is served. For instance, the pair of users $\mathcal{K}_{\tilde{k}_1} = \{k = 1, 5\}$ and $\mathcal{K}_{\tilde{k}_2} = \{k = 2, 4\}$ can reuse the same supersymbol, which corresponds to a reusing factor of 2 for both sets.

The supersymbols for the resulting connectivity graphs are shown in Fig. 10. It can be easily seen that there are not enough dimensions to align the interference of the 3 connectivity graphs simultaneously according to the BIA criterion. In order to provide enough signal dimensions, the supersymbol of the graph $\mathcal{Q}_2$ is expanded 3 times so that the Block 1 of the graph $\mathcal{Q}_3$ can be transmitted over a period in which the preset mode of the users of $\mathcal{Q}_2$ remains constant as is shown in Fig. 11. The resulting supersymbol can be divided into super-block 1 (S-Block 1) where simultaneous transmission occurs and super-Block 2 (S-Block 2) in which each symbol is transmitted in a dedicated symbol extension. The supersymbol construction can be easily determined treating

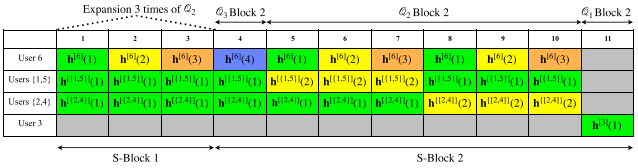

FIGURE 11. Supersymbol of the KM-topBIA scheme for the toy example.

the expansion as the left-hand of a Kronecker product. During S-Block 1 the resulting pattern for the user $\tilde{k}_q$ at the connectivity graph $\mathcal{Q}_2$ is given by $f_{\text{S-B1}}^{[\tilde{k}_q,2]} = f_{\text{B1}}^{[\tilde{k}_q,2]} \otimes \mathbf{1}_3$, where $f_{\text{B1}}^{[\tilde{k}_q,q]}$ is the correlation function of the sBIA scheme during Block 1 for the user $\tilde{k}_q$ of the graph q. Moreover, due to this expansion, the resulting supersymbol provides 3 alignment blocks per each user belonging to $\mathcal{Q}_2$, which occupy a dedicated symbol extension of Block 2 each. The graph $\mathcal{Q}_1$ contains a user connected to a single transmitter, i.e., $\tilde{L}_q = 1$, whose supersybmbol only contains a Block 2 section (see Fig.10(c)).

Notice that the resulting signal transmission does not change for the connectivity graph $\mathcal{Q}_3$ during its Block 1. Similarly to the supersymbol construction, the signal transmitted in $\mathcal{Q}_2$ can be also managed using the Kronecker product. Denoting the precoding matrix of the sBIA for $\mathcal{Q}_2$ for the user $\tilde{k}_q$ during Block 2 as $\mathbf{W}_{\text{B1}}^{[\tilde{k}_q,q]}$, the resulting precoding matrix during S-Block 1 is $\mathbf{W}_{\text{S-B1}}^{[\tilde{k}_q,q]} = \mathbf{W}_{\text{B1}}^{[\tilde{k}_q,q]} \otimes \mathbf{I}_3$. Therefore, the transmitted signal during S-Block 1 for the graph $\mathcal{Q}_2$ is given by

$$\mathbf{X}_{\text{S-B1}}^{[\mathcal{Q}_2]} = \sum_{\tilde{k}_2=1}^{\tilde{K}_2} \mathbf{W}_{\text{S-B1}}^{[k_2,2]} \mathbf{u}_T^{[\mathcal{K}_{\tilde{k}_2}]} \tag{23}$$

where $\mathbf{u}_T^{[\mathcal{K}_{\tilde{k}_2}]} = \text{col}\left\{\mathbf{u}_\ell^{[\mathcal{K}_{\tilde{k}_2}]}\right\}_{\ell=1}^{3}$ contains the symbols transmitted during the 3 alignment blocks obtained after the expansion carried out in $\mathcal{Q}_2$ and $\mathbf{u}_\ell^{[\mathcal{K}_{\tilde{k}_2}]} = \left[\mathbf{u}_\ell^{[\mathcal{K}_{\tilde{k}_2}(1)]}, \ldots, \mathbf{u}_\ell^{[\mathcal{K}_{\tilde{k}_2}(\eta_{\tilde{k}_2})]}\right]$ contains the symbols to the K_2 users of the graph $\mathcal{Q}_2$.

Once the S-Block 1 has been determined, the design of S-Block 2 results straightforward. Each alignment block of each user completes the last symbol extension during S-Block 2. Thus, as it is shown in Fig. 11, the user $k = 6$ belonging to $\mathcal{Q}_3$ selects the preset mode $\mathbf{h}(4)$ during the symbol extension 4. Since the symbol associated to this alignment block is transmitted in a dedicated symbol extension, all other users can measure the interference because of its transmission during the symbol extensions $\{1, 2, 3\}$. Similarly, a dedicated symbol extension per each alignment block of $\mathcal{Q}_2$ is allocated during the symbol extensions $\{5, 6, 7\}$ and $\{8, 9, 10\}$ at the preset mode $\mathbf{h}(2)$ where the corresponding symbol is transmitted in orthogonal fashion. Since the proposed supersymbol satisfies the BIA criterion the interference because of transmission in $\mathcal{Q}_2$ can me measured in $\mathcal{Q}_3$ and subtracted afterwards. Furthermore, transmission for connectivity graphs composed

of a single transmitter, i.e., $\tilde{L}_q = 1$ requieres a dedicated symbol extension in S-Block 2. Thus, transmission to the user $k = 3$ is carried out during the symbol extension 11 and it does not generate or receive interference to or from other users.

The achievable sum-DoF per symbol extension for the connectivity graphs $\mathcal{Q}_1$, $\mathcal{Q}_2$ and $\mathcal{Q}_3$ are equal to $\frac{1}{11}$, $\frac{2\times2\times3\times2}{11}$ and $\frac{4}{11}$, respectively. Therefore, the sum-DoF of the whole cluster is $\frac{29}{11} \approx 2.63$. It is interesting to remark that the KM-sBIA scheme can achieve 2.66 DoF for the considered cluster, i.e., both schemes obtain almost the same sum-DoF. However, the KM-sBIA requires 2187 symbol extensions while the KM-topBIA supersymbol comprises 11 symbol extensions. Furthermore, and even more important, KM-topBIA adapts to the connectivity of each user maximizing the usefulness of each transmitter and reducing the noise increase.

C. GENERAL CASE

For the general case, the key idea of the KM-topBIA scheme is based on expanding and repeating the sBIA structure for each graph of connectivity. The flow chart of the proposed KM-topBIA scheme is depicted in Fig. 12. In the following, we provide a systematic procedure to obtain the supersymbol structure and precoding matrices.

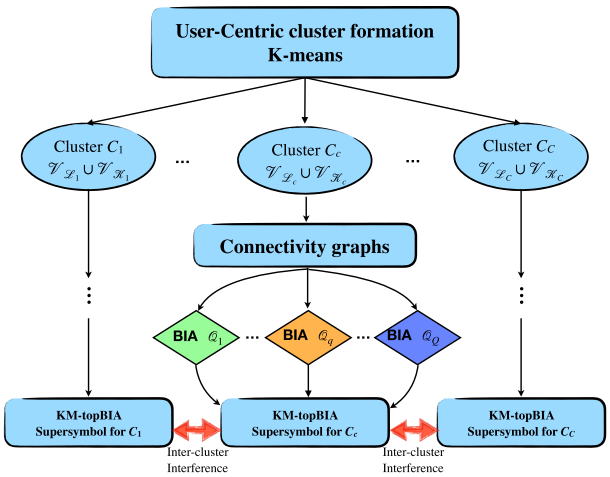

FIGURE 12. Flow chart of the KM-topBIA scheme.

1) CONNECTIVITY GRAPHS AND REUSING FACTOR

Each cluster c contains users with distinct connectivity. Taking into consideration the set of users connected to the same number of transmitters, Q connectivity graphs are obtained as described above for the toy example. For the sake of an easy explanation, the connectivity of the graphs is sorted in ascending order, i.e., $\tilde{L}_q > \tilde{L}_{q-1}$. Although each connectivity graph contains L_q transmitters and K_q users, the supersymbol structure and the transmitted signal is determined by the connectivity of each graph and the number of users that cannot reuse the same pattern denoted as $\tilde{L}_q$ and $\tilde{K}_q$, respectively. Thus, each user $\tilde{k}_q$, which can be treated as a virtual user of multiple users that can reuse the same pattern, comprises the set of users $\mathcal{K}_{\tilde{k}_q} = \left\{\mathcal{K}_{\tilde{k}_q}(1), \ldots, \mathcal{K}_{\tilde{k}_q}(\eta_{\tilde{k}_q})\right\}$. Moreover, the total reusing gain of the connectivity graph q is defined as $\Omega_q = \frac{K_q}{\tilde{K}_q}$.

2) CONSTRUCTION OF S-BLOCK 1 FOR KM-TOPBIA

For connectivity graphs $\tilde{L}_q > 1$ the KM-topBIA scheme comprises a S-Block 1 by expanding and repeating the structure of the sBIA scheme. First, it is necessary to ensure the alignment of the Q connectivity graphs of the cluster. To do so, the channel state of the users with lower connectivity must remain constant while the users with a greater connectivity modify their preset modes in order to implement the alignment block structure of the corresponding sBIA scheme as is shown in Fig. 13. That is, the resulting expansion of the Block 1 for the graph q must provide enough signal dimensions to align the signal space of the graphs with greater connectivity. For instance, the supersymbol of the group q must be expanded $(L_{q-1} - 1)^{K_{q-1}-1}$ times to guarantee the alignment of the connectivity graph with connectivity q regarding the graph with connectivity $q-1$. Following this procedure recursively, the superymbol of the graph q is expanded

$$E_q = \prod_{q'=q+1,\ \tilde{L}_{q'}\neq 1}^{Q} (\tilde{L}_{q'} - 1)^{\tilde{K}_{q'}} \tag{24}$$

times. Hence, considering the connectivity graph with the lowest connectivity, the S-Block 1 comprises

$$\Lambda_{\text{S-B1}} = \prod_{q=1,\ \tilde{L}_q\neq 1}^{Q} (\tilde{L}_q - 1)^{\tilde{K}_q} \tag{25}$$

symbol extensions. As a consequence of this expansion, the connectivity graphs $q' > q$ can repeat their pattern $(\tilde{L}_q - 1)^{\tilde{K}_q}$ times. This methodology is depicted in Fig. 13. Similarly as the expansion described above, following the repetition procedure recursively, the pattern of preset modes of each user belonging to the connectivity graph q is repeated

$$R_q = \prod_{q'=1,\ \tilde{L}_{q'}\neq 1}^{q-1} (\tilde{L}_{q'} - 1)^{\tilde{K}_{q'}} \tag{26}$$

times. Therefore, the resulting pattern of preset modes, i.e., the supersymbol, of the user $\tilde{k}_q$ can be obtained considering the repetition R_q and the expansion E_q as the left and right hand of the Kronecker product, respectively. That is,

$$f_{\text{B1}}^{[\tilde{k}_q,q]} = \mathbf{1}_{R_q} \otimes f_{\text{S-B1}}^{[\tilde{k}_q,q]} \otimes \mathbf{1}_{E_q}. \tag{27}$$

Once the supersymbol structure has been defined, the precoding matrices of the KM-topBIA scheme are obtained following the same steps of repetition and expansion described above. The resulting precoding matrices of KM-topBIA in S-Block 1 are given by

$$\mathbf{W}_{\text{S-B1}}^{[\tilde{k}_q,q]} = \mathbf{I}_{R_q} \otimes \mathbf{W}_{\text{B1}}^{[\tilde{k}_q,q]} \otimes \mathbf{I}_{E_q}. \tag{28}$$

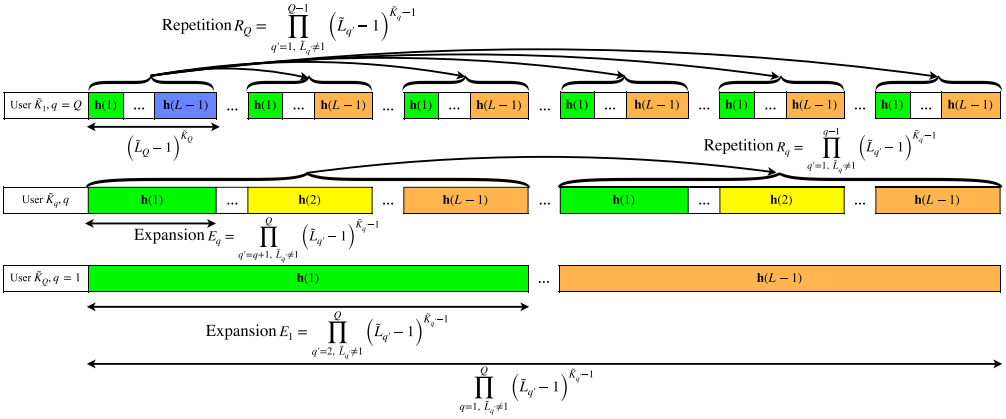

FIGURE 13. S-Block 1 construction for the general case of the KM-topBIA scheme.

Notice that the proposed strategy increases $E_q R_q$ times the number of alignment blocks allocated to each user. Thus, the proposed scheme provides $N_q = E_q R_q (\tilde{L}_q - 1)^{\tilde{K}_q - 1}$ alignment blocks to each user of the connectivity graph q. Therefore, the signal transmitted during S-Block 1 by the L_q transmitters of the connectivity graph q is

$$\mathbf{X}_{\text{S-B1}}^{[\mathcal{Q}_q]} = \sum_{k=1}^{\tilde{K}_q} \mathbf{W}_{\text{S-B1}}^{[\tilde{k}_q,q]} \mathbf{u}_T^{[\mathcal{K}_{\tilde{k}_q}]}, \tag{29}$$

where $\mathbf{X}_{\text{S-B1}}^{[\mathcal{Q}_q]} = \text{col}\left\{\mathbf{x}^{[\mathcal{Q}_q]}[n]\right\}_{n=1}^{\Lambda_{\text{S-B1}}}$, $\mathbf{x}^{[\mathcal{Q}_q]}[n]$ is the signal transmitted by the L_q transmitters of the connectivity cluster q at time n and $\mathbf{u}_T^{[\mathcal{K}_{\tilde{k}_q}]} = \text{col}\left\{\mathbf{u}_\ell^{[\mathcal{K}_{\tilde{k}_q}]}\right\}_{\ell=1}^{N_q}$. Taking into consideration the reusing factor $\eta_{\tilde{k}_q}$ of each virtual user

$$\mathbf{u}_\ell^{[\mathcal{K}_{\tilde{k}_q}]} = \left[\mathbf{u}_\ell^{[\mathcal{K}_{\tilde{k}_q}(1)]} \ \ldots \ \mathbf{u}_\ell^{[\mathcal{K}_{\tilde{k}_q}(\eta_{\tilde{k}_q})]} \ \mathbf{0}_{L_q - \tilde{L}_q \eta_{\tilde{k}_q}, 1}\right]. \tag{30}$$

Each symbol $\mathbf{u}_\ell^{[\mathcal{K}_{\tilde{k}_q}]}$ contains the symbols given by the reuse factor and a possible padding for the cases where there are not users that can reuse the corresponding supersymbol.

3) CONSTRUCTION OF S-BLOCK 2 AND INTERFERENCE REMOVAL

During S-Block 2 a dedicated symbol extension per alignment block of each user at any connectivity graph Q is provided to complete each alignment block and allow the measurement of the interference because of transmission to other users. Moreover, transmission to the users with connectivity $\tilde{L}_q = 1$ only occurs in S-Block 2. Notice that these users are not affected by the repetition and the expansion procedure described above. We consider that each of the K_{q_0} users belonging to a connectivity graph with $\tilde{L}_q = 1$ can be repeated κ times. Since there are $E_q R_q (\tilde{L}_q - 1)^{\tilde{K}_q - 1}$ alignment blocks for each user of the graph q, the S-Block 2 comprises

$$\Lambda_{\text{S-B2}} = \sum_{q=1}^{Q} \tilde{K}_q E_q R_q (\tilde{L}_q - 1)^{\tilde{K}_q - 1} + \kappa \tilde{K}_{q_0} \tag{31}$$

symbol extensions. For the users with $\tilde{L}_q > 1$, the S-Block 2 is divided into $\sum_{q=1}^{Q} \tilde{K}_q$ blocks where each virtual user $\tilde{k}_q$ completes each alignment block. Specifically, the user $\tilde{k}_q$ of the connectivity graph q selects the preset mode $\tilde{L}_q$ at the following symbol extensions

$$\left\{\Lambda_{\text{S-B1}} + (\tilde{k}_q - 1) \sum_{q=1}^{Q} E_q R_q \left(\tilde{L}_q - 1\right)^{\tilde{K}_q - 1} + \ell\right\}_{\ell=1}^{N_q}, \tag{32}$$

$\tilde{k}_q = \{1, \ldots, \tilde{K}_q\}$. Since the symbol $\mathbf{u}_\ell^{[\tilde{k}_q]}$ is transmitted in a dedicated symbol extension during the last element of its ℓ-th alignment block, the transmission of $\mathbf{u}_\ell^{[\tilde{k}_q]}$ in S-Block 2 is allocated in the block column ℓ of the precoding matrix of the user k. For the users with connectivity $\tilde{L}_q = 1$ transmission occurs during the following $\kappa \tilde{K}_{q_0}$ symbols extensions. To conclude the construction of S-Block 2 each user $\tilde{k}_q$ of the connectivity graph q selects the preset mode that corresponds to the mode selected at the symbol extensions polluted by the transmission of $\mathbf{u}_\ell^{[\mathcal{K}_{\tilde{k}'_q}]}$, $\tilde{k}'_q \neq \tilde{k}_q$ for $q = \{1, \ldots, Q\}/\tilde{L}_q \neq 1$. Since the proposed KM-topBIA supersymbol satisfies the BIA criterion, the interference because of transmission of $\mathbf{u}_\ell^{[\mathcal{K}_{\tilde{k}'_q}]}$ is aligned in a single preset mode.

4) ACHIEVABLE DOF AND USER RATE FOR KM-TOPBIA

For the general case, the supersymbol of the KM-topBIA comprises

$$\Lambda_{\text{KM-topBIA}} = \prod_{q=1}^{Q} \left(\tilde{L}_q - 1\right)^{\tilde{K}_q} + \sum_{q=1}^{Q} \tilde{K}_q N_q + \kappa \tilde{K}_{q_0} \tag{33}$$

symbol extensions. Since each user of the group q obtains N_q alignment blocks containing $\tilde{L}_q$ DoF each and taking into consideration the reusing factor, after some rearranging,

the achievable sum-DoF of the cluster of interest c is

$$\mathrm{DoF}^{[c]}_{\mathrm{KM-topBIA}} = \sum_{q=1,\,\tilde{L}_q\neq 1}^{Q} \frac{\Omega_q \tilde{L}_q \tilde{K}_q}{\tilde{L}_q + \tilde{K}_q - 1} + \frac{\kappa \tilde{K}_{q_0}}{\Lambda_{\mathrm{KM-topBIA}}}. \tag{34}$$

Notice that in contrast to other BIA-based schemes (see (16) and (18)) the achievable sum-DoF of the KM-topBIA is given by the connectivity of each user.

Similarly to the KM-sBIA scheme the inter-cluster interference is treated as noise. Thus, the signal after interference subtraction follows the same structure as (20). However, the channel matrix of the user $\tilde{k}_q$ belonging to the graph q contains only components given by the connectivity of the user. Therefore, the achievable rate of the user $k \in \mathcal{K}_{\tilde{k}_q}$ belonging to the cluster c is given by

$$R^{[k,q,c]}_{\mathrm{KM-topBIA}} = B_q \mathbb{E}\left[\log\det\left(\mathbf{I} + P_{\mathrm{str}} \mathbf{H}^{[k,q]}_c \mathbf{H}^{[k,q]H}_c \tilde{\mathbf{R}}^{-1}_{z_I}\right)\right], \tag{35}$$

where B_q is the ratio of alignment blocks per supersymbol length for the considered user, $\mathbf{H}^{[k,q]}_c$ is the channel matrix of the user k belonging to the connectivity graph q of the cluster c and the covariance matrix of the interference plus noise is

$$\tilde{\mathbf{R}}_{z_I} = \tilde{\mathbf{R}}_z + P_{\mathrm{led}} \sum_{k'\in\mathcal{K}_{\tilde{k}_q}, k'\neq k}^{\eta_q} \mathbf{H}^{[k]}_{\mathcal{L}_{\tilde{k}_q}(k')} \mathbf{H}^{[k]H}_{\mathcal{L}_{\tilde{k}_q}(k')} + P_{\mathrm{led}} \sum_{c'=1, c'\neq c}^{C} \mathbf{H}^{[k]}_{c'} \mathbf{H}^{[k]H}_{c'} \tag{36}$$

and

$$\tilde{\mathbf{R}}_z = \begin{bmatrix} \sum_{q=1, q\notin\tilde{L}_q=1}^{Q} \tilde{K}_q \mathbf{I}_{\tilde{L}_q - 1} & 0 \\ 0 & 1 \end{bmatrix}. \tag{37}$$

In (36), $\mathbf{H}^{[k]}_{\mathcal{L}_{\tilde{k}_q}(k')}$ is the channel matrix between the $\tilde{L}_q$ transmitters of the graph q that reuse the same pattern and the user of interest k and $\mathbf{H}^{[k]}_{c'}$ is the channel matrix between the cluster c', $c' \neq c$, and the user k.

VII. SIMULATION RESULTS

We now present the simulation results for characterizing the derived BIA-based UC schemes in comparison with other BIA schemes, a TPC scheme such as ZF and MRC treating the reconfigurable photodetector as an angle diversity receiver. The reconfigurable photodetector provides $M = 16$ preset modes according to a pyramidal arrangement with $\theta_{\mathrm{pyr}} = 30°$. We consider an indoor scenario with a size 15 m × 15 m × 3 m in which a 4 × 4 LED transmitters are distributed uniformly over the ceiling while the users are randomly distributed in a plane with a height 2.15 m to the ceiling. If a parameter is not specified, its value is listed in Table 1.

TABLE 1. Simulation Parameters.

Parameter	Value
Optical transmission power P_{led}	10 W
Bandwidth for VLC AP	20 MHz
Physical area of the photodiode A	15 mm2
Transmitter semi-angle $\phi_{1/2}$	60 deg
Receiver FOV φ_F	70 deg
Coefficient of the photodiode r	70 deg
Detector responsivity δ	0.53 A/W
Gain of optical filter and concentrator $g()$	1.0
Noise power spectral density σ^2_n	$10^{-22} A^2$/Hz
Number of clusters for NC approach C	4

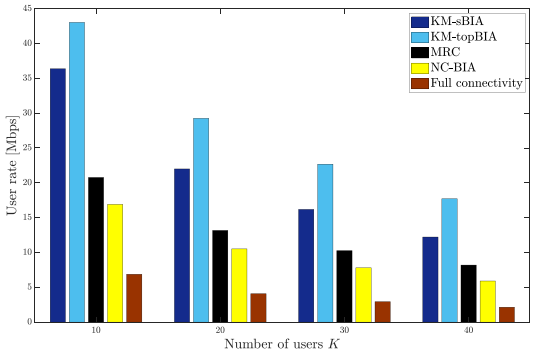

FIGURE 14. Average user rate of KM-sBIA and KM-topBIA for distinct FoV values in comparison with MRC, NC-BIA and sBIA assuming full connectivity in the whole network. $K = 20$.

A. USER RATE ANALYSIS

The achievable user rate of the considered schemes for distinct number of users is depicted in Fig. 14. First, it can be seen that the proposed KM-sBIA and KM-topBIA schemes achieve higher user rates than the BIA-based NC approach or MRC. Specially, for a reduced number of users, e.g. $K = 10$ or $K = 20$, the proposed schemes multiply by two the user rate achieved by the NC approach. Furthermore, applying a sBIA scheme managing the VLC network as a full connectivity system, i.e., as a single BC, obtains a poor user rate almost 5 times lower than the KM-topBIA scheme.

In Fig. 15 we analyze the user rate regarding the number of clusters considered in the proposed clustering strategy. This analysis comprises from a whole network approach, i.e., $c = 0$, to a single transmitter clustering, i.e., $c = L$. Notice that the relation between the user-rate and the number of clusters determines the amount of inter-cluster interference and the noise increase because of interference subtraction (see (36) and (37)). For both schemes, KM-sBIA and KM-topBIA, it can be seen that there exists an optimal value of the number of clusters. Specifically, the optimal number of clusters for KM-sBIA and KM-topBIA is 5 and 3, respectively.

The achievable user rate for an optical power from -5 dBW to 15 dBW is depicted in Fig. 16. It can be seen that both

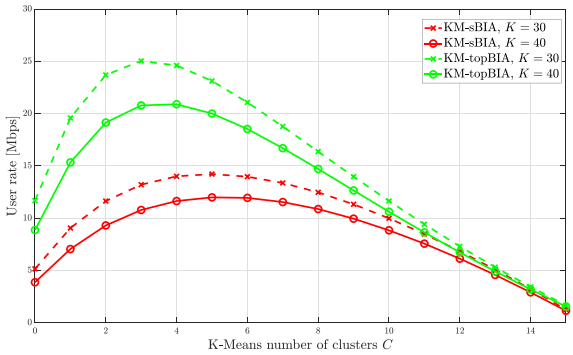

FIGURE 15. Average user rate for KM-sBIA and KM-topBIA regarding the number of clusters.

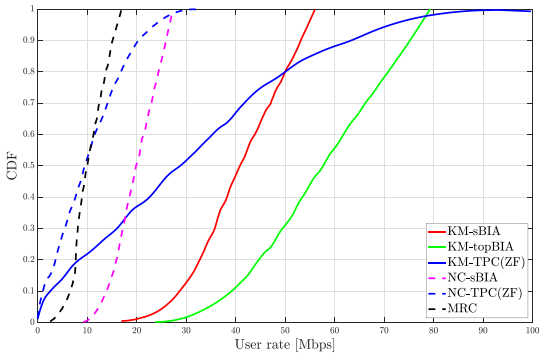

FIGURE 17. CDF of the user rate for the considered schemes based on NC and UC approaches.

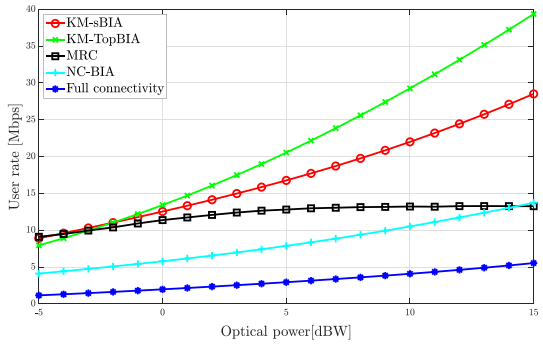

FIGURE 16. Average user rate for KM-sBIA and KM-topBIA versus the transmitted optical power in comparison with MRC, NC-BIA and sBIA assuming full connectivity in the whole network. $K = 20$.

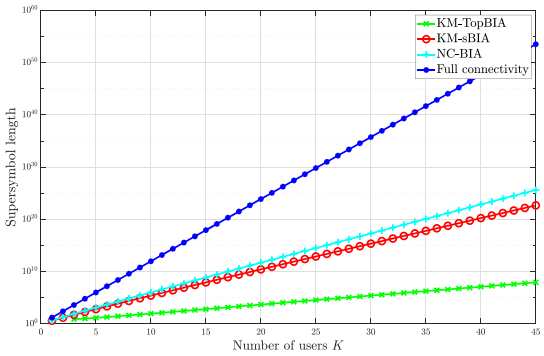

FIGURE 18. Comparison of the supersymbol lengths for the considered BIA approaches.

schemes, BIA-based on a NC approach and assuming full connectivity, obtain a poor user rate as the optical power increases since they are subject to a strong interference, either from inter-cluster interference or due to interference subtraction, respectively. For diversity schemes such as MRC the user rate does not increase beyond an optical power of 5 dBW because the interference increases proportionally to the power. The proposed schemes outperform the aforementioned schemes. Moreover, the user rate of KM-topBIA is characterized by a greater slope than KM-sBIA since it adapts to the connectivity of each user.

The cumulative distribution function (CDF) of the proposed KM-sBIA and KM-topBIA schemes in comparison with the considered schemes is shown Fig. 17. First, it can be seen that the NC approach and the MRC scheme achieve lower user rate than any scheme based on a UC design. Considering a UC clustering strategy for the implementation of a TPC scheme such as ZF improves the user rate considerably. However, notice that ZF obtains a user rate distribution with a great variance where the percentile 50^{th} corresponds to a user rate below 30 Mbps. In this sense, KM-sBIA and KM-topBIA schemes achieve a user rate greater than 30 Mbps and 40 Mbps, respectively, at the percentile 10^{th} of the CDF. In other words, the proposed schemes guarantee a user rate above 30 Mbps for most of the cases.

B. SUPERSYMBOL LENGTH

Since the VLC networks are not subject to small scale effects, the coherence of the physical channel is given by the users mobility, which must remain constant during the transmission of the entire supersymbol. In Fig. 18, the length of the supersymbol is depicted for the proposed KM-sBIA and KM-topBIA schemes in comparison with a full connectivity and NC-BIA. Since the supersymbol length increases exponentially regarding the number of transmitters and users, the full connectivity approach generates supersymbols with a non-suitable length for any realistic implementation. The NC-sBIA and KM-sBIA schemes reduce considerably the supersymbol length since the network is divided into several clusters. Moreover, notice that the supersymbol length results similar for both KM-sBIA and NC-BIA since KM-sBIA considers values around $C = 4$ (see Fig. 15), and therefore, the main difference is due to the users distribution, which is averaged through several simulations. In this sense, it can be seen that KM-topBIA generates the shortest supersymbols, and therefore, the requirements on coherence, i.e., on the users mobility, are relaxed.

In Fig. 19, the supersymbol length is depicted as a function of the number of clusters for the KM-sBIA and the KM-topBIA schemes considering $\{30, 40\}$ users. As expected, increasing the number of clusters leads to

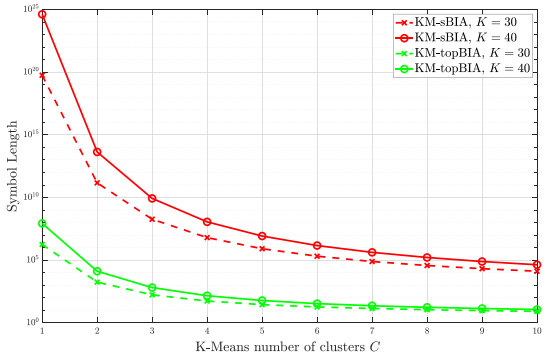

FIGURE 19. The effect of Clusters number on the supersymbol lengths for the BIA approaches based on the KM-algorithm.

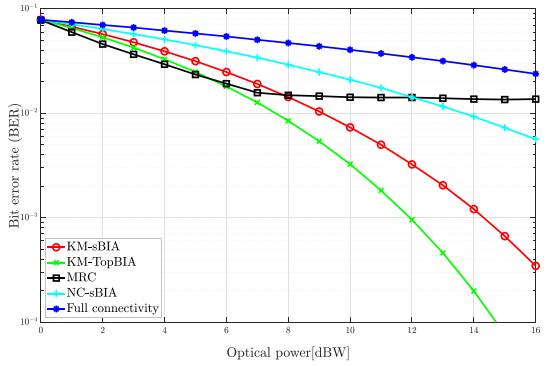

FIGURE 20. BER for 2-PAM Modulation.

shorter supersymbol. Indeed, for both schemes the supersymbol length corresponds to a reasonable value for a realistic implementation considering the optimal value of the number of clusters (see Fig. 15).

C. BIT ERROR RATE

In Fig. 20, we plot the BER for $K = 20$ users for an optical power of each transmitter in the range of (0, 16) dBW. The symbols are transmitted using a 2-PAM. First, it is interesting to remark that applying sBIA considering full connectivity in the whole network provides a BER above 10^{-2} in that range of optical power due to the noise increase because of the interference subtraction of the whole set of users. Considering a NC approach the BER improves regarding the full connectivity case. However, the BER is barely below 10^{-2} for 16 dBW. It can be seen that the proposed UC schemes improve the BER considerably. Specifically, a BER of $2 \cdot 10^{-4}$ and 10^{-3} is achieved for an optical power of 14 dBW for the KM-sBIA and KM-topBIA schemes, respectively.

VIII. CONCLUSIONS

In this work, we propose a UC network design to facilitate the use of BIA schemes in VLC systems based on the concept of reconfigurable photodetector. The UC design is based on the K-means clustering algorithm employing the topology of the network. Given the proposed clustering strategy we derive both a scheme that manages each cluster as a BC referred to as KM-sBIA and a novel scheme that exploits the topology of each cluster combining BIA schemes according to the connectivity of each user referred to as KM-topBIA. In comparison with other BIA schemes they both provide greater user rate comprising shorter coherence blocks. The proposed schemes outperform TPC schemes such as ZF for both NC and UC approaches. Managing the reconfigurable photodetector as an angle diversity receiver they also obtain greater user rate than diversity schemes such as MRC. Moreover, both schemes obtain lower BER than the aforementioned ZF and MRC schemes. Furthermore, the KM-topBIA outperforms KM-sBIA in terms of rate and BER while requiring shorter coherence blocks since it adapts to the connectivity of each user.

REFERENCES

[1] C.-X. Wang *et al.*, "Cellular architecture and key technologies for 5G wireless communication networks," *IEEE Commun. Mag.*, vol. 52, no. 2, pp. 122–130, Feb. 2014.

[2] S. Al-Ahmadi, O. Maraqa, M. Uysal, and S. M. Sait, "Multi-user visible light communications: State-of-the-art and future directions," *IEEE Access*, vol. 6, pp. 70555–70571, 2018.

[3] C. Chen, D. A. Basnayaka, and H. Haas, "Downlink performance of optical attocell networks," *J. Lightw. Technol.*, vol. 34, no. 1, pp. 137–156, Jan. 1, 2016.

[4] L. Zeng *et al.*, "High data rate multiple input multiple output (MIMO) optical wireless communications using white led lighting," *IEEE J. Sel. Areas Commun.*, vol. 27, no. 9, pp. 1654–1662, Dec. 2009.

[5] D. Gesbert, S. Hanly, H. Huang, S. S. Shitz, O. Simeone, and W. Yu, "Multi-cell MIMO cooperative networks: A new look at interference," *IEEE J. Sel. Areas Commun.*, vol. 28, no. 9, pp. 1380–1408, Dec. 2010.

[6] N. Zhao, F. R. Yu, M. Jin, Q. Yan, and V. C. M. Leung, "Interference alignment and its applications: A survey, research issues, and challenges," *IEEE Commun. Surveys Tuts.*, vol. 18, no. 3, pp. 1779–1803, 3rd Quart., 2016.

[7] H. Sifaou, A. Kammoun, K.-H. Park, and M.-S. Alouini, "Robust transceivers design for multi-stream multi-user MIMO visible light communication," *IEEE Access*, vol. 5, pp. 26387–26399, 2017.

[8] H. Marshoud, D. Dawoud, V. M. Kapinas, G. K. Karagiannidis, S. Muhaidat, and B. Sharif, "MU-MIMO precoding for VLC with imperfect CSI," in *Proc. 4th Int. Workshop Opt. Wireless Commun. (IWOW)*, Sep. 2015, pp. 93–97.

[9] T. V. Pham, H. Le-Minh, and A. T. Pham, "Multi-user visible light communication broadcast channels with zero-forcing precoding," *IEEE Trans. Commun.*, vol. 65, no. 6, pp. 2509–2521, Jun. 2017.

[10] Y. Hong, J. Chen, Z. Wang, and C. Yu, "Performance of a precoding MIMO system for decentralized multiuser indoor visible light communications," *IEEE Photon. J.*, vol. 5, no. 4, Aug. 2013, Art. no. 7800211.

[11] H. Elgala, R. Mesleh, and H. Haas, "An LED model for intensity-modulated optical communication systems," *IEEE Photon. Technol. Lett.*, vol. 22, no. 11, pp. 835–837, Jun. 1, 2010.

[12] T. Fath and H. Haas, "Performance comparison of MIMO techniques for optical wireless communications in indoor environments," *IEEE Trans. Commun.*, vol. 61, no. 2, pp. 733–742, Feb. 2013.

[13] S. A. Jafar, "Blind interference alignment," *IEEE J. Sel. Topics Signal Process.*, vol. 6, no. 3, pp. 216–227, Jun. 2012.

[14] T. Gou, C. Wang, and S. A. Jafar, "Aiming perfectly in the dark-blind interference alignment through staggered antenna switching," *IEEE Trans. Signal Process.*, vol. 59, no. 6, pp. 2734–2744, Jun. 2011.

[15] M. Morales-Céspedes, J. Plata-Chaves, D. Toumpakaris, S. A. Jafar, and A. G. Armada, "Blind interference alignment for cellular networks," *IEEE Trans. Signal Process.*, vol. 63, no. 1, pp. 41–56, Jan. 2015.

[16] Y. Lu, W. Zhang, and K. B. Letaief, "Blind interference alignment with diversity in$k$-user interference channels," *IEEE Trans. Commun.*, vol. 62, no. 8, pp. 2850–2859, Aug. 2014.

[17] H. Yang, W. Shin, and J. Lee, "Hierarchical blind interference alignment over interference networks with finite coherence time," *IEEE Trans. Signal Process.*, vol. 64, no. 5, pp. 1289–1304, Mar. 2016.

[18] M. Morales-Céspedes, M. C. Paredes-Paredes, A. G. Armada, and L. Vandendorpe, "Aligning the light without channel state information for visible light communications," *IEEE J. Sel. Areas Commun.*, vol. 36, no. 1, pp. 91–105, Jan. 2018.
[19] A. Nuwanpriya, S.-W. Ho, and C. S. Chen, "Indoor MIMO visible light communications: Novel angle diversity receivers for mobile users," *IEEE J. Sel. Areas Commun.*, vol. 33, no. 9, pp. 1780–1792, Sep. 2015.
[20] Z. Chen, D. A. Basnayaka, X. Wu, and H. Haas, "Interference mitigation for indoor optical attocell networks using an angle diversity receiver," *J. Lightw. Technol.*, vol. 36, no. 18, pp. 3866–3881, Sep. 15, 2018.
[21] I. Chih-Lin, C. Rowell, S. Han, Z. Xu, G. Li, and Z. Pan, "Toward green and soft: A 5G perspective," *IEEE Commun. Mag.*, vol. 52, no. 2, pp. 66–73, Feb. 2014.
[22] R. Zhang, J. Wang, Z. Wang, Z. Xu, C. Zhao, and L. Hanzo, "Visible light communications in heterogeneous networks: Paving the way for user-centric design," *IEEE Wireless Commun.*, vol. 22, no. 2, pp. 8–16, Apr. 2015.
[23] X. Li, R. Zhang, J. Wang, and L. Hanzo, "Cell-centric and user-centric multi-user scheduling in visible light communication aided networks," in *Proc. IEEE Int. Conf. Commun. (ICC)*, Jun. 2015, pp. 5120–5125.
[24] X. Li, R. Zhang, and L. Hanzo, "Optimization of visible-light optical wireless systems: Network-centric versus user-centric designs," *IEEE Commun. Surveys Tuts.*, pp. 1878–1904, 3rd Quart., 2018.
[25] X. Li, F. Jin, R. Zhang, J. Wang, Z. Xu, and L. Hanzo, "Users first: User-centric cluster formation for interference-mitigation in visible-light networks," *IEEE Trans. Wireless Commun.*, vol. 15, no. 1, pp. 39–53, Jan. 2016.
[26] J. M. Kahn and J. R. Barry, "Wireless infrared communications," *Proc. IEEE*, vol. 85, no. 2, pp. 265–298, Feb. 1997.
[27] T. Komine and M. Nakagawa, "Fundamental analysis for visible-light communication system using LED lights," *IEEE Trans. Consum. Electron.*, vol. 50, no. 1, pp. 100–107, Feb. 2004.
[28] Y. Wang, X. Wu, and H. Haas, "Load balancing game with shadowing effect for indoor hybrid LiFi/RF networks," *IEEE Trans. Wireless Commun.*, vol. 16, no. 4, pp. 2366–2378, Apr. 2017.
[29] X. Li, R. Zhang, and L. Hanzo, "Cooperative load balancing in hybrid visible light communications and WiFi," *IEEE Trans. Commun.*, vol. 63, no. 4, pp. 1319–1329, Apr. 2015.
[30] L. Bottou and Y. Bengio, "Convergence properties of the k-means algorithms," in *Advances in Neural Information Processing Systems*. Cambridge, MA, USA: MIT Press, 1995, pp. 585–592.

AHMAD ADNAN-QIDAN (S'18) received the B.Sc. degree in laser and optoelectronics engineering from Al-Nahrain University, Baghdad, Iraq, in 2012, and the M.Sc. degree in laser/electronic and communication engineering from the Institute of Laser for Postgraduate Studies, University of Baghdad, Baghdad, Iraq, in 2015. He is currently pursuing the Ph.D. degree in multimedia and communications with the Universidad Carlos III de Madrid, Madrid, Spain. His research interests include visible light communication, interference management, and hybrid networking.

MÁXIMO MORALES CÉSPEDES (S'10–M'15) was born in Valdepeñas, Ciudad Real, Spain, in 1986. He received the B.Sc., M.Sc., and Ph.D. degrees from the Universidad Carlos III de Madrid, Spain, in 2010, 2012, and 2015, respectively, all in electrical engineering, with a specialization in multimedia and communications. In 2012, he was a finalist of the IEEE Region 8 Student Paper Contest. From 2015 to 2017, he was a Postdoctoral Fellow with the Institute of Information and Communication Technologies, Electronics and Applied Mathematics, Universite Catholique de Louvain. He is currently with the Department of Signal Theory and Communications, Universidad Carlos III de Madrid. His research interests include interference management, visible light communications, hardware implementations, MIMO techniques, and signal processing applied to wireless communications.

ANA GARCÍA ARMADA (S'96–A'98–M'00–SM'08) received the Ph.D. degree in electrical engineering from the Polytechnical University of Madrid, in 1998. She has been a Visiting Scholar with Stanford University, Bell Labs, and the University of Southampton. She is currently a Professor with the Universidad Carlos III de Madrid, Spain, where she held a variety of management positions (the Head of the Signal Theory and Communications Department, the Vice Dean of electrical engineering, the Deputy Vice-Chancellor of international relations, among others), where she is also leading the Communications Research Group. She has participated in more than 30 national and ten international research projects and 20 contracts with the industry, all of them related to wireless communications. She has co-authored eight book chapters on wireless communications and signal processing. She has published around 150 papers in international journals and conference proceedings and she holds four patents. She has contributed to international standards organizations such as ITU and ETSI. Her current interests include multi-carrier and multi-antenna techniques and signal processing applied to wireless communications. She is a member of the expert group of the European 5G PPP. She was a recipient of the Young Researchers Excellence Award and the Award to Best Practices in Teaching from the University Carlos III of Madrid. She serves on the Editorial Boards of *Physical Communication*, *IET Communications*, and the IEEE COMMUNICATIONS LETTERS.